

## Long-term optical-infrared color variability of blazars

Bing-Kai Zhang<sup>1</sup>, Xiao-Shan Zhou<sup>1</sup>, Xiao-Yun Zhao<sup>1</sup> and Ben-Zhong Dai<sup>2</sup>

<sup>1</sup> Department of Physics, Fuyang Normal College, Fuyang 236041, China; [zhangbk@ihep.ac.cn](mailto:zhangbk@ihep.ac.cn)

<sup>2</sup> Department of Physics, Yunnan University, Kunming 650091, China

Received 2014 November 9; accepted 2015 April 3

**Abstract** The long-term optical and infrared color variability of blazars has been investigated with monitoring data from the Small and Moderate Aperture Research Telescope System (SMARTS). The sample in this study consists of 49 flat spectrum radio quasars (FSRQs) and 22 BL Lacertae objects (BL Lacs). The fractional variability amplitudes of each source have been calculated in both optical *R* band and infrared *J* band. Overall, the variability amplitudes of FSRQs are larger than those of BL Lacs. The results also suggest that the variability amplitude of most FSRQs is larger at a lower energy band (*J* band) than at a higher one (*R* band), but the variability amplitude of BL Lacs is larger at the higher energy band. Both types of blazars display color variation along with variability in brightness. However, they show different variation behaviors in general. In the whole data set, 35 FSRQs exhibit redder-when-brighter trends, and 11 FSRQs exhibit opposite trends; 11 BL Lacs follow bluer-when-brighter trends, and seven BL Lacs follow opposite trends. A detailed examination indicates that there are 10 blazars showing redder-when-brighter trends in their low state, and bluer-when-brighter or stable-when-brighter trends in their high state. Some more complicated color behaviors have also been detected in several blazars. The non-thermal jet emission and the thermal emission from the accretion disk are employed to explain the observed color behaviors.

**Key words:** galaxies: active — BL Lacertae objects: general — quasars: general — methods: statistical

### 1 INTRODUCTION

Blazars consist of flat spectrum radio quasars (FSRQs) and BL Lacertae objects (BL Lacs). They are dominated by non-thermal continuum emission. The flux decreases with the frequency increasing, which approximately follows a power law. Measurements of their spectral energy distribution (SED) play an important role in understanding the emission processes of blazars. Since blazars vary rapidly and violently at all wavelengths from radio to  $\gamma$ -ray with time scales from minutes to years (Carini et al. 1992; Arévalo et al. 2008; Ghosh et al. 2000; Ciprini et al. 2007; Chatterjee et al. 2012; Zhang et al. 2013; D’Ammando et al. 2013), the lack of simultaneous data at various wavelengths is an obstacle in the broadband study of blazars. Flux variations in blazars are usually accompanied by changes in the spectral shape. Therefore, the analysis of spectral changes of blazars can put some strong constraints on the physical processes that are responsible for these variations.

The spectral changes can be characterized by color variations. Color variations in blazars have been explored by several authors. For 28 radio-selected BL Lacs in Fan & Lin (2000), two showed flatter spectra when getting brighter, while three showed opposite behavior. Vagnetti et al. (2003) found bluer-when-brighter (BWB) trends in the *BVRI* bands for all eight BL Lacs in their sample. Gu et al. (2006) found that three out of five BL Lacs exhibited significant BWB trends and two out of three FSRQs exhibited redder-when-brighter (RWB) trends. However, Gu & Ai (2011) showed that only one FSRQ is RWB in a sample of 29 SDSS FSRQs. Rani et al. (2010) found that three out of six BL Lacs tended to become bluer with an increase in brightness, and four out of six FSRQs exhibited opposite trends. Ikejiri et al. (2011) found that 28 out of 32 well observed blazars showed a BWB trend. Bonning et al. (2012) found that FSRQs had redder optical-infrared colors when they were brighter, but BL Lac objects showed no such trend. Gaur et al. (2012) suggested that six out of ten BL Lacs followed the BWB trend, but all six BL Lacs in Sandrinelli et al. (2014) showed no BWB trends. The color behaviors of some individual sources have also been investigated in many diverse literatures (Raiteri et al. 2003; Papadakis et al. 2003; Hu et al. 2006; Wu et al. 2006, 2011; Dai et al. 2009; Zhang et al. 2010a; Dai et al. 2011; Fan et al. 2014).

BWB and RWB trends are two common well-observed behaviors in blazars. However, some complicated color phenomena have also been found in some cases. In general, there are five kinds of color behaviors: BWB in whole data sets; RWB in whole data sets; cycles or loop-like patterns; RWB in the low state while BWB in the high state (RWB to BWB); stable-when-brighter (SWB) or no correlation with brightness in whole data sets (see Zhang et al. 2014 and references therein). Up to now, FSRQs and BL Lacs seem not to have universal features in color variations. The purpose of this paper is to investigate their color behaviors using a much larger sample of blazars with almost simultaneous measurements, and we expect to provide results with higher confidence levels. The paper is organized as follows: in Section 2, the infrared and optical data as well as their variations are described; in Section 3, the color behavior is studied; then the discussion and conclusions are given in Section 4.

## 2 INFRARED AND OPTICAL DATA AND THEIR VARIABILITY

In order to investigate the statistics of the color behavior of blazars, we compile data from 71 blazars and four possible blazars from sources acquired by the Small and Moderate Aperture Research Telescope System (SMARTS). The SMARTS program employs four meter-class telescopes (1.5-m, 1.3-m, 1.0-m and 0.9-m) at Cerro Tololo Interamerican Observatory (CTIO) in Chile to observe the bright southern gamma-ray blazars on a regular cadence, at both optical and near-infrared wavelengths. Data reduction and analysis of SMARTS data have been described in Bonning et al. (2012).

Table 1 lists our sample which is comprised of 49 FSRQs, 22 BL Lacs and four unidentified type sources. The first column gives the object name, the second column gives the spectral classification, the third one gives the monitoring duration in days, and the fourth one gives the number of data points for color index calculation. Most of these sources are observed in *B*, *V*, *R*, *J* and *K* bands. On the whole, there are the most data points in *R* and *J* bands. So, these two bands have been selected to study color variations. However, the observations for each source are not uniform. Some objects have been observed for more than 2000 days, while some others have been observed for less than 100 days. Some sources have been well observed with hundreds of data points and some have less than 10 data points.

In order to compare the amplitude of the variations in different blazars, and in different bands for the same blazar, we compute the fractional variability amplitude  $F_{\text{var}}$  (Vaughan et al. 2003), which represents the average amplitude of the observed variations as a percentage of the mean of a light curve. The fractional variability amplitude is defined as  $F_{\text{var}} = \sqrt{(S^2 - \langle \varepsilon_{\text{err}}^2 \rangle) / \langle x \rangle^2}$ , where  $S^2$  is the sample variance of the light curve,  $\langle x \rangle$  is the average flux and  $\langle \varepsilon_{\text{err}}^2 \rangle$  is the mean squared error. The  $F_{\text{var}}$  values of *J* and *R* bands are listed in the fifth and sixth columns of Table 1 respectively.

**Table 1** Properties Associated with Variations of Optical and Infrared Data

Object	Class	$\Delta T$	$N$	$F_{\text{var}, J}$	$F_{\text{var}, R}$	$r_{J-R}$	Prob.	$r_{C-R}$	Prob.	$r_{C-J}$	Prob.	Behavior
(1)	(2)	(3)	(4)	(5)	(6)	(7)	(8)	(9)	(10)	(11)	(12)	(13)
PMN 0017–0512	FSRQ	211	73	0.82±0.07	0.67±0.06	0.97	< 10 <sup>-9</sup>	0.67	< 10 <sup>-11</sup>	0.82	< 10 <sup>-9</sup>	RWB
PKS 0035–252	FSRQ	357	9	0.43±0.11	0.38±0.10	0.11	0.78	-0.49	0.18	0.81	8.0 × 10 <sup>-3</sup>	RWB
PKS 0208–512	FSRQ	2016	381	0.96±0.03	0.86±0.03	0.96	< 10 <sup>-9</sup>	0.30	2.7 × 10 <sup>-9</sup>	0.55	< 10 <sup>-9</sup>	RWB
4C+01.02	FSRQ	76	8	0.32±0.08	0.17±0.04	0.73	0.04	0.34	0.40	0.89	2.7 × 10 <sup>-3</sup>	RWB
AO 0235+164	FSRQ	1816	221	1.57±0.07	1.59±0.08	0.98	< 10 <sup>-9</sup>	0.21	2.1 × 10 <sup>-3</sup>	0.38	4.2 × 10 <sup>-9</sup>	RWB
PKS 0235–618	FSRQ	158	14	0.25±0.05	0.32±0.06	0.48	0.09	-0.72	3.9 × 10 <sup>-3</sup>	0.27	0.35	BWB
1RXS 0238–3116	BL Lac	654	20	0.20±0.03	0.29±0.05	-0.10	0.68	-0.87	7.7 × 10 <sup>-7</sup>	0.58	7.2 × 10 <sup>-3</sup>	BWB(RWB)
PKS 0250–225	FSRQ	90	50	0.40±0.04	0.40±0.04	0.85	< 10 <sup>-9</sup>	-0.26	0.07	0.29	0.04	None
PKS 0301–243	BL Lac	537	48	0.15±0.02	0.18±0.02	0.84	< 10 <sup>-9</sup>	-0.56	4.1 × 10 <sup>-5</sup>	-0.02	0.89	BWB
BG6 J0316+0904	BL Lac	783	12	0.16±0.03	0.25±0.05	0.92	2.3 × 10 <sup>-5</sup>	-0.82	9.7 × 10 <sup>-4</sup>	-0.54	0.07	BWB
PKS 0402–362	FSRQ	863	75	0.26±0.02	0.17±0.01	0.86	< 10 <sup>-9</sup>	0.34	2.5 × 10 <sup>-3</sup>	0.78	< 10 <sup>-9</sup>	RWB
PMN 0413–5332	FSRQ	763	11	0.48±0.12	0.10±0.06	-0.26	0.44	-0.49	0.12	0.97	9.0 × 10 <sup>-7</sup>	RWB
PKS 0422+004	BL Lac	498	11	0.42±0.09	0.44±0.09	0.99	1.5 × 10 <sup>-8</sup>	-0.28	0.40	-0.13	0.71	None
PKS 0426–380	FSRQ	419	163	0.35±0.02	0.34±0.02	0.92	< 10 <sup>-9</sup>	-0.18	0.02	0.22	4.9 × 10 <sup>-3</sup>	RWB
NRAO 190	FSRQ	236	15	0.86±0.16	0.77±0.14	0.94	1.7 × 10 <sup>-7</sup>	0.32	0.24	0.62	0.01	RWB
PKS 0454–234	FSRQ	847	286	0.61±0.03	0.68±0.03	0.99	< 10 <sup>-9</sup>	-0.62	< 10 <sup>-9</sup>	-0.48	< 10 <sup>-9</sup>	BWB
PKS 0454–46	FSRQ	1193	47	0.14±0.02	0.15±0.02	0.21	0.16	-0.61	5.6 × 10 <sup>-6</sup>	0.65	8.5 × 10 <sup>-7</sup>	RWB(BWB)
S3 0458–02	FSRQ	496	39	0.34±0.04	0.31±0.04	0.93	< 10 <sup>-9</sup>	0.12	0.45	0.48	1.9 × 10 <sup>-3</sup>	RWB
PKS 0502+049	FSRQ	309	36	0.52±0.06	0.34±0.04	0.76	9.4 × 10 <sup>-8</sup>	0.01	0.97	0.66	1.2 × 10 <sup>-5</sup>	RWB
PMN 0507–6104	FSRQ	816	6	0.61±0.18	0.66±0.19	0.75	0.09	-0.25	0.64	0.46	0.36	None
PKS 0528+134	FSRQ	2091	160	0.54±0.03	0.31±0.02	0.78	< 10 <sup>-9</sup>	0.23	4.1 × 10 <sup>-3</sup>	0.79	< 10 <sup>-9</sup>	RWB
PMN J0531–4827	—	1215	175	0.94±0.05	1.01±0.05	0.98	< 10 <sup>-9</sup>	-0.34	3.6 × 10 <sup>-6</sup>	-0.13	0.09	BWB
PKS 0537–441	FSRQ	1115	141	0.77±0.05	0.66±0.04	0.97	< 10 <sup>-9</sup>	0.16	0.05	0.40	1.1 × 10 <sup>-6</sup>	RWB
PMN J0623+3350	—	61	20	0.40±0.07	0.54±0.09	0.75	1.2 × 10 <sup>-4</sup>	-0.67	1.2 × 10 <sup>-3</sup>	-0.02	0.93	BWB
J0630.9–2406	BL Lac	827	18	0.21±0.04	0.12±0.02	0.37	0.14	-0.26	0.30	0.81	5.5 × 10 <sup>-5</sup>	RWB
PKS 0637–75	FSRQ	1193	72	0.09±0.01	0.07±0.01	0.30	0.01	-0.46	5.7 × 10 <sup>-5</sup>	0.72	< 10 <sup>-9</sup>	RWB(BWB)
PKS 0727–11	FSRQ	989	18	0.64±0.12	0.88±0.15	0.96	< 10 <sup>-9</sup>	-0.86	4.1 × 10 <sup>-6</sup>	-0.69	1.7 × 10 <sup>-3</sup>	BWB
PMN J0816–1311	BL Lac	843	21	0.22±0.03	0.23±0.04	0.97	< 10 <sup>-9</sup>	-0.36	0.10	-0.11	0.62	None
PKS 0818–128	BL Lac	826	20	0.23±0.04	0.36±0.06	0.53	0.02	-0.76	1.1 × 10 <sup>-4</sup>	0.16	0.51	BWB
BZQ J0850–1213	FSRQ	1206	97	0.55±0.04	0.53±0.04	0.91	< 10 <sup>-9</sup>	-0.21	0.04	0.21	0.04	None
OJ 287	BL Lac	2203	364	0.42±0.02	0.41±0.02	0.92	< 10 <sup>-9</sup>	-0.04	0.49	0.35	< 10 <sup>-9</sup>	RWB
PKS 1004–217	FSRQ	1087	81	0.20±0.02	0.14±0.01	-0.12	0.29	-0.72	< 10 <sup>-9</sup>	0.77	< 10 <sup>-9</sup>	RWB(BWB)
PKS 1056–113	BL Lac	728	43	0.37±0.04	0.43±0.05	0.97	< 10 <sup>-9</sup>	-0.35	0.02	-0.10	0.52	None
PKS 1124–186	FSRQ	351	34	0.34±0.04	0.34±0.04	1.00	< 10 <sup>-9</sup>	0.54	9.5 × 10 <sup>-6</sup>	0.60	2.0 × 10 <sup>-4</sup>	RWB
PKS 1127–14	FSRQ	1103	37	0.21±0.03	0.17±0.02	-0.12	0.49	-0.62	4.6 × 10 <sup>-5</sup>	0.85	< 10 <sup>-9</sup>	RWB(BWB)
PKS 1144–379	FSRQ	1115	128	0.56±0.04	0.65±0.04	0.93	< 10 <sup>-9</sup>	-0.66	< 10 <sup>-9</sup>	-0.34	6.9 × 10 <sup>-5</sup>	BWB
QSO B1212+078	BL Lac	942	9	0.07±0.02	0.12±0.03	0.47	0.21	-0.78	0.01	0.18	0.63	BWB
3C 273	FSRQ	2156	287	0.06±0.00	0.04±0.00	0.14	0.02	-0.54	< 10 <sup>-9</sup>	0.76	< 10 <sup>-9</sup>	RWB(BWB)
PKS 1244–255	FSRQ	1032	107	0.55±0.04	0.48±0.03	0.98	< 10 <sup>-9</sup>	0.69	< 10 <sup>-9</sup>	0.81	< 10 <sup>-9</sup>	RWB
3C 279	FSRQ	2207	447	0.68±0.02	0.72±0.02	0.99	< 10 <sup>-9</sup>	-0.46	< 10 <sup>-9</sup>	-0.33	< 10 <sup>-9</sup>	BWB
PKS 1329–049	FSRQ	376	11	0.24±0.08	0.48±0.11	0.08	0.82	-0.73	0.01	0.62	0.04	BWB
PKS 1335–127	FSRQ	1077	54	0.91±0.09	0.87±0.08	0.95	< 10 <sup>-9</sup>	0.10	0.47	0.42	1.6 × 10 <sup>-3</sup>	RWB
PKS B1406–076	FSRQ	2201	180	0.61±0.03	0.44±0.02	0.80	< 10 <sup>-9</sup>	0.14	0.06	0.71	< 10 <sup>-9</sup>	RWB
PKS B1424–418	FSRQ	765	278	0.71±0.03	0.74±0.03	0.99	< 10 <sup>-9</sup>	-0.38	< 10 <sup>-9</sup>	-0.26	1.3 × 10 <sup>-5</sup>	BWB
PKS 1508–05	FSRQ	745	25	0.20±0.03	0.10±0.02	0.25	0.22	-0.27	0.20	0.86	2.7 × 10 <sup>-8</sup>	RWB
PKS 1510–089	FSRQ	2207	405	0.96±0.03	0.85±0.03	0.96	< 10 <sup>-9</sup>	0.53	< 10 <sup>-9</sup>	0.74	< 10 <sup>-9</sup>	RWB
PKS 1514–241	BL Lac	1065	68	0.15±0.01	0.15±0.01	0.81	< 10 <sup>-9</sup>	-0.27	0.03	0.35	3.1 × 10 <sup>-3</sup>	RWB
PKS 1550–242	—	304	17	0.55±0.10	0.57±0.10	0.97	< 10 <sup>-9</sup>	-0.23	0.38	0.00	1.00	None
PMN J1610–6649	BL Lac	741	16	0.19±0.03	0.16±0.03	0.97	< 10 <sup>-9</sup>	0.53	0.03	0.72	1.8 × 10 <sup>-3</sup>	RWB

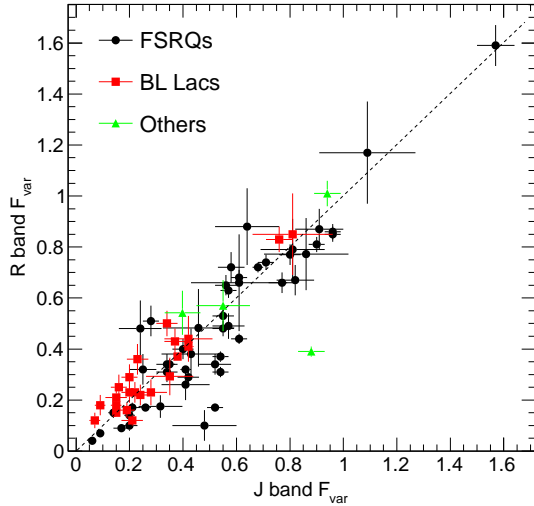
**Table 1** — *Continued.*

Object	Class	$\Delta T$	$N$	$F_{\text{var}, J}$	$F_{\text{var}, R}$	$\tau_{J-R}$	Prob.	$r_{C-R}$	Prob.	$r_{C-J}$	Prob.	Behavior
(1)	(2)	(3)	(4)	(5)	(6)	(7)	(8)	(9)	(10)	(11)	(12)	(13)
PKS 1622-253	FSRQ	988	6	0.46±0.13	0.48±0.15	0.74	0.09	-0.03	0.95	0.65	0.16	RWB
PKS 1622-297	FSRQ	2165	221	0.54±0.03	0.37±0.02	0.85	< 10 <sup>-9</sup>	0.27	4.9 × 10 <sup>-5</sup>	0.74	< 10 <sup>-9</sup>	RWB
1717-5156	—	455	133	0.88±0.05	0.39±0.02	0.86	< 10 <sup>-9</sup>	0.59	< 10 <sup>-9</sup>	0.92	< 10 <sup>-9</sup>	RWB
PKS 1730-130	FSRQ	1985	243	0.41±0.02	0.32±0.01	0.79	< 10 <sup>-9</sup>	-0.05	0.39	0.57	< 10 <sup>-9</sup>	RWB
OT 081	BL Lac	379	14	0.81±0.15	0.85±0.16	0.99	< 10 <sup>-9</sup>	-0.33	0.25	-0.19	0.51	None
PMN J1921-1607	BL Lac	543	13	0.28±0.06	0.23±0.05	0.96	2.3 × 10 <sup>-7</sup>	0.63	0.02	0.82	5.6 × 10 <sup>-4</sup>	RWB
PKS 1954-388	FSRQ	1118	54	0.42±0.04	0.29±0.03	0.96	< 10 <sup>-9</sup>	0.72	< 10 <sup>-9</sup>	0.88	< 10 <sup>-9</sup>	RWB
PKS 1958-179	FSRQ	919	18	1.09±0.18	1.17±0.20	0.98	< 10 <sup>-9</sup>	-0.59	0.01	-0.42	0.08	BWB
PKS 2052-474	FSRQ	1553	176	0.80±0.04	0.77±0.04	0.96	< 10 <sup>-9</sup>	0.10	0.18	0.39	7.8 × 10 <sup>-8</sup>	RWB
2FGL J2055.4-0023	BL Lac	752	11	0.15±0.04	0.21±0.05	-0.29	0.38	-0.83	1.4 × 10 <sup>-3</sup>	0.77	5.4 × 10 <sup>-3</sup>	BWB(RWB)
PKS 2142-75	FSRQ	1316	157	0.52±0.03	0.17±0.01	0.88	< 10 <sup>-9</sup>	0.77	< 10 <sup>-9</sup>	0.98	< 10 <sup>-9</sup>	RWB
PKS 2149-306	FSRQ	158	22	0.17±0.03	0.09±0.01	0.92	2.0 × 10 <sup>-9</sup>	0.72	1.7 × 10 <sup>-4</sup>	0.94	< 10 <sup>-9</sup>	RWB
PKS 2155-304	BL Lac	1940	363	0.38±0.01	0.37±0.01	0.99	< 10 <sup>-9</sup>	0.06	0.29	0.22	1.7 × 10 <sup>-5</sup>	RWB
3C 446	BL Lac	1111	56	0.34±0.04	0.50±0.05	0.35	7.3 × 10 <sup>-3</sup>	-0.60	9.8 × 10 <sup>-7</sup>	0.53	2.2 × 10 <sup>-5</sup>	BWB(RWB)
PKS 2227-08	FSRQ	915	43	0.28±0.03	0.51±0.06	0.32	0.04	-0.87	< 10 <sup>-9</sup>	0.18	0.24	BWB
PKS 2232-488	FSRQ	661	10	0.41±0.09	0.26±0.06	0.66	0.04	0.02	0.96	0.76	0.01	RWB
PKS 2233-148	BL Lac	507	122	0.76±0.05	0.83±0.05	1.00	< 10 <sup>-9</sup>	-0.53	< 10 <sup>-9</sup>	-0.45	2.6 × 10 <sup>-7</sup>	BWB
PKS 2240-260	BL Lac	1147	20	0.24±0.04	0.22±0.04	0.92	1.1 × 10 <sup>-8</sup>	0.22	0.35	0.59	6.6 × 10 <sup>-3</sup>	RWB
3C 454.3	FSRQ	1985	505	0.90±0.03	0.81±0.03	0.99	< 10 <sup>-9</sup>	0.76	< 10 <sup>-9</sup>	0.85	< 10 <sup>-9</sup>	RWB
PKS 2255-282	FSRQ	947	42	0.57±0.06	0.49±0.05	0.94	< 10 <sup>-9</sup>	0.26	0.09	0.58	6.6 × 10 <sup>-5</sup>	RWB
1ES 2322-409	BL Lac	809	19	0.20±0.03	0.23±0.04	0.96	< 10 <sup>-9</sup>	-0.58	9.1 × 10 <sup>-3</sup>	-0.33	0.17	BWB
PKS 2326-502	FSRQ	128	76	0.58±0.05	0.72±0.06	0.97	< 10 <sup>-9</sup>	-0.56	1.8 × 10 <sup>-7</sup>	-0.35	2.2 × 10 <sup>-3</sup>	BWB
PMN 2345-1555	FSRQ	790	167	0.57±0.03	0.63±0.03	0.98	< 10 <sup>-9</sup>	-0.40	1.1 × 10 <sup>-7</sup>	-0.19	0.01	BWB
PKS 2345-16	FSRQ	372	22	0.81±0.12	0.79±0.12	-0.97	< 10 <sup>-9</sup>	-0.99	< 10 <sup>-9</sup>	0.99	< 10 <sup>-9</sup>	RWB(BWB)
H 2356-309	BL Lac	478	10	0.09±0.02	0.18±0.04	0.69	0.03	-0.83	3.1 × 10 <sup>-3</sup>	-0.16	0.65	BWB
4C+01.28	BL Lac	27	8	0.35±0.09	0.29±0.07	-0.95	3.5 × 10 <sup>-4</sup>	-0.99	4.6 × 10 <sup>-6</sup>	0.99	7.2 × 10 <sup>-6</sup>	BWB(RWB)

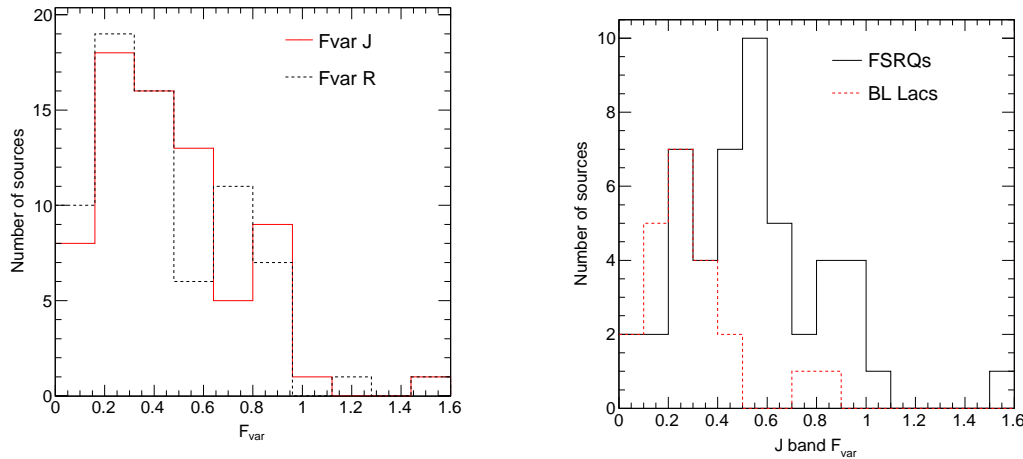
In Figure 1 we plot the  $F_{\text{var}}$  of  $R$  band versus that of  $J$  band for each object. It can be seen that the objects show great differences in variations. Most of the objects show significant variabilities. Several sources display extreme variability, such as AO 0235-164, with  $F_{\text{var}}=1.57$  in  $J$  band and  $F_{\text{var}}=1.59$  in  $R$  band. However, there are also a few sources showing weak variabilities, such as 3C 273, with  $F_{\text{var}}=0.06$  in  $J$  band and  $F_{\text{var}}=0.04$  in  $R$  band.

Figure 2 plots the distribution of  $F_{\text{var}}$  values of the  $R$  band and  $J$  band. On the whole,  $F_{\text{var}}$  values of the  $R$  band have no significant difference with those of the  $J$  band for all objects, which means that the variability amplitudes of the  $R$  and  $J$  bands in blazars are comparable. Ghosh et al. (2000) suggested that it may not be correct to generalize that the amplitude of the variation in blazars is systematically larger at higher frequency. However, as can be seen in Figure 1,  $F_{\text{var}}$  values of the  $J$  band are generally larger than those of the  $R$  band for most of the FSRQs (with prob. = 0.025), while  $F_{\text{var}}$  values of the  $J$  band are, in general, smaller than those of  $R$  band for most of the BL Lacs (with prob. = 0.033). Bonning et al. (2012) also found that eight out of nine FSRQs are more variable in  $J$  band than in  $B$  band. As can also be seen in Figure 1, the  $F_{\text{var}}$  values of FSRQs seem to be larger than those of BL Lacs.

Figure 3 displays the  $F_{\text{var}}$  distribution of FSRQs and BL Lacs in  $J$  band. One can clearly see that  $J$  band  $F_{\text{var}}$  values of FSRQs are larger than those of BL Lacs. The difference is significant at a level of  $5.7 \times 10^{-4}$ .



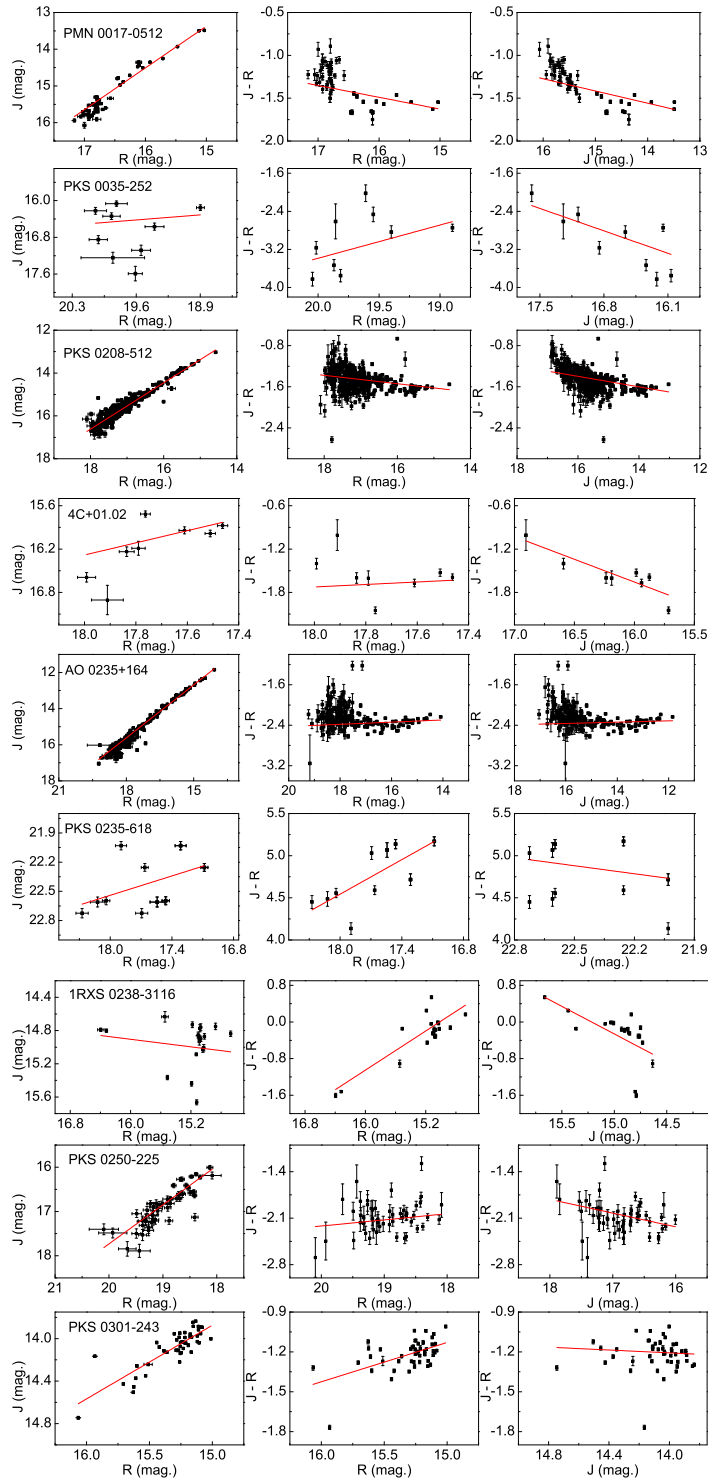
**Fig. 1**  $F_{\text{var}}$  values of  $R$  band versus those of  $J$  band. The dots, squares and triangles represent FSRQs, BL Lacs and unidentified type objects, respectively. The dashed line means that the  $F_{\text{var}}$  of  $J$  band is equal to that of  $R$  band.



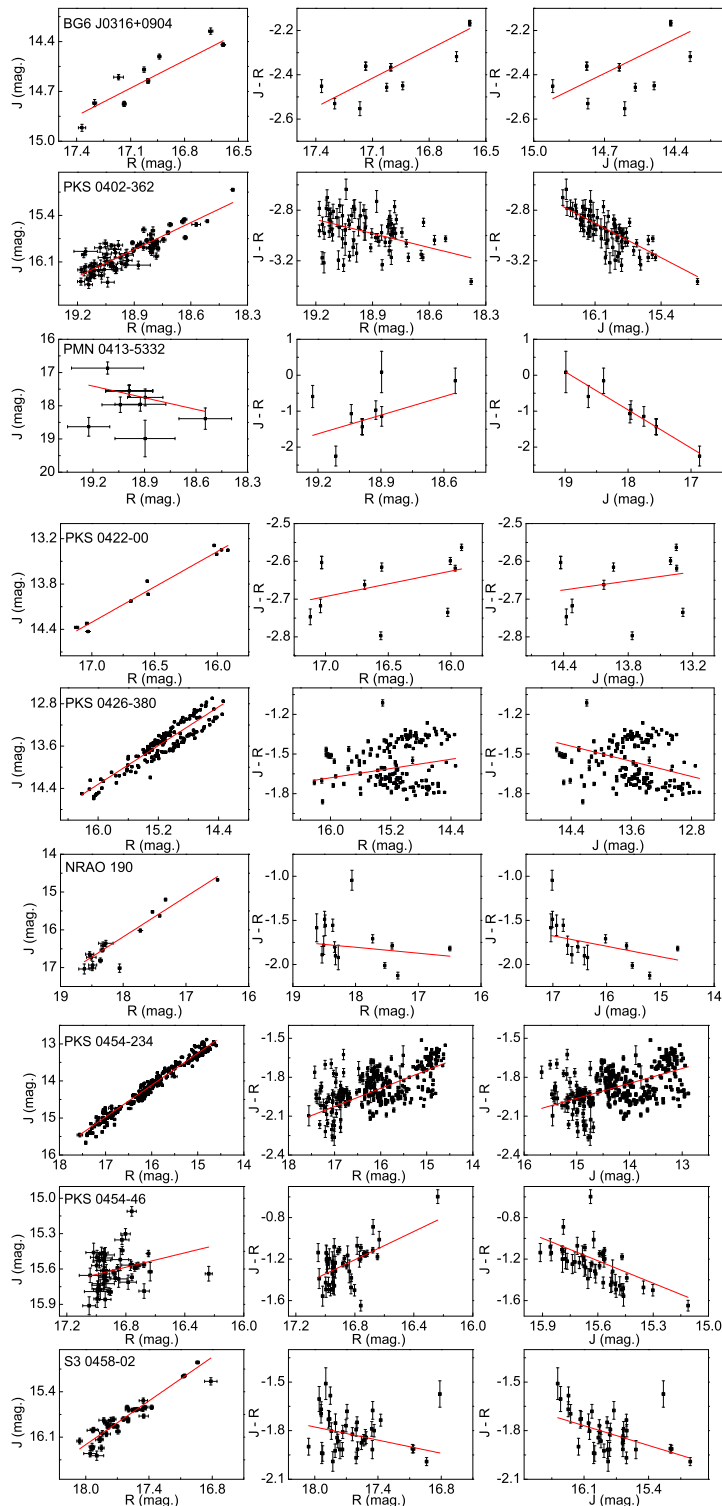
**Fig. 2** Distributions of  $F_{\text{var}}$  values of the optical  $R$  band (dashed line) and the infrared  $J$  band (solid line).

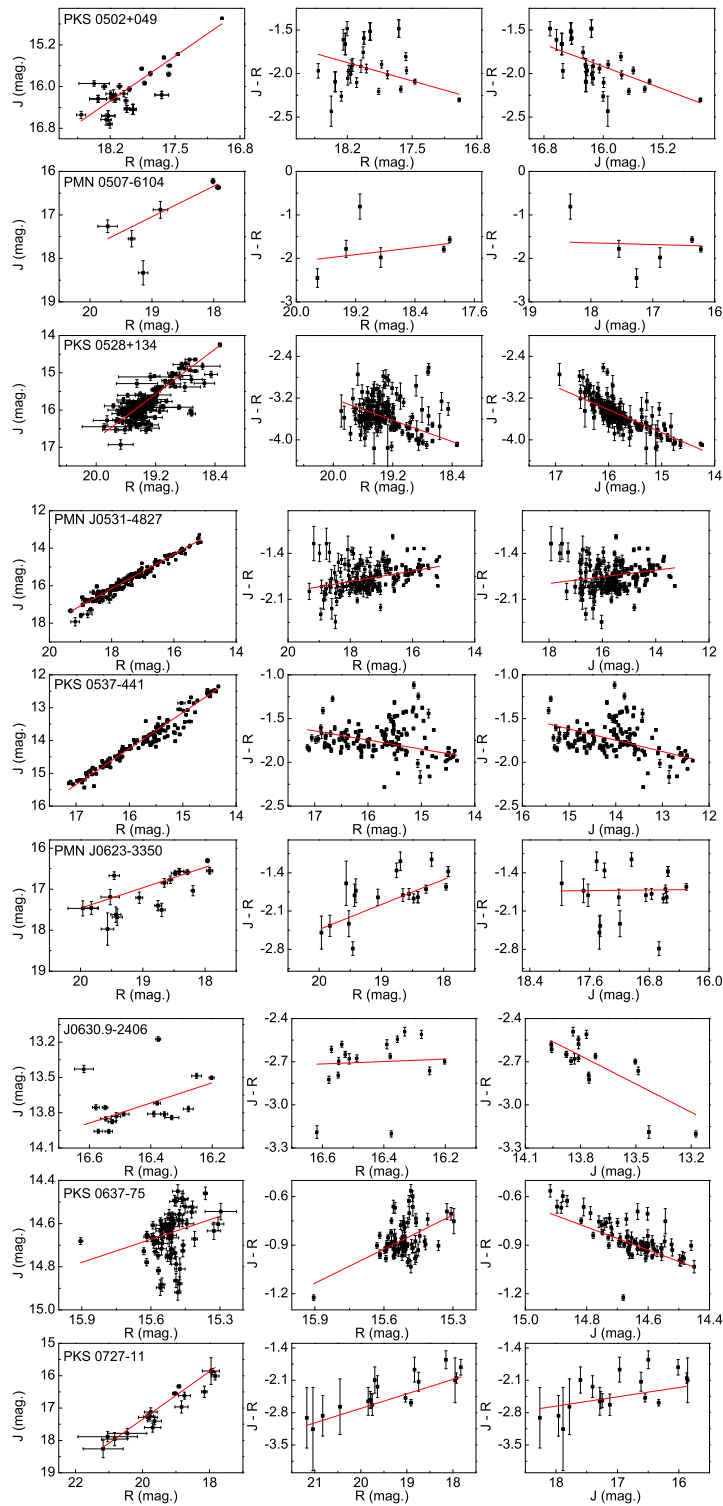
**Fig. 3** Distributions of  $J$  band  $F_{\text{var}}$  values of FSRQs (solid line) and BL Lacs (dashed line).

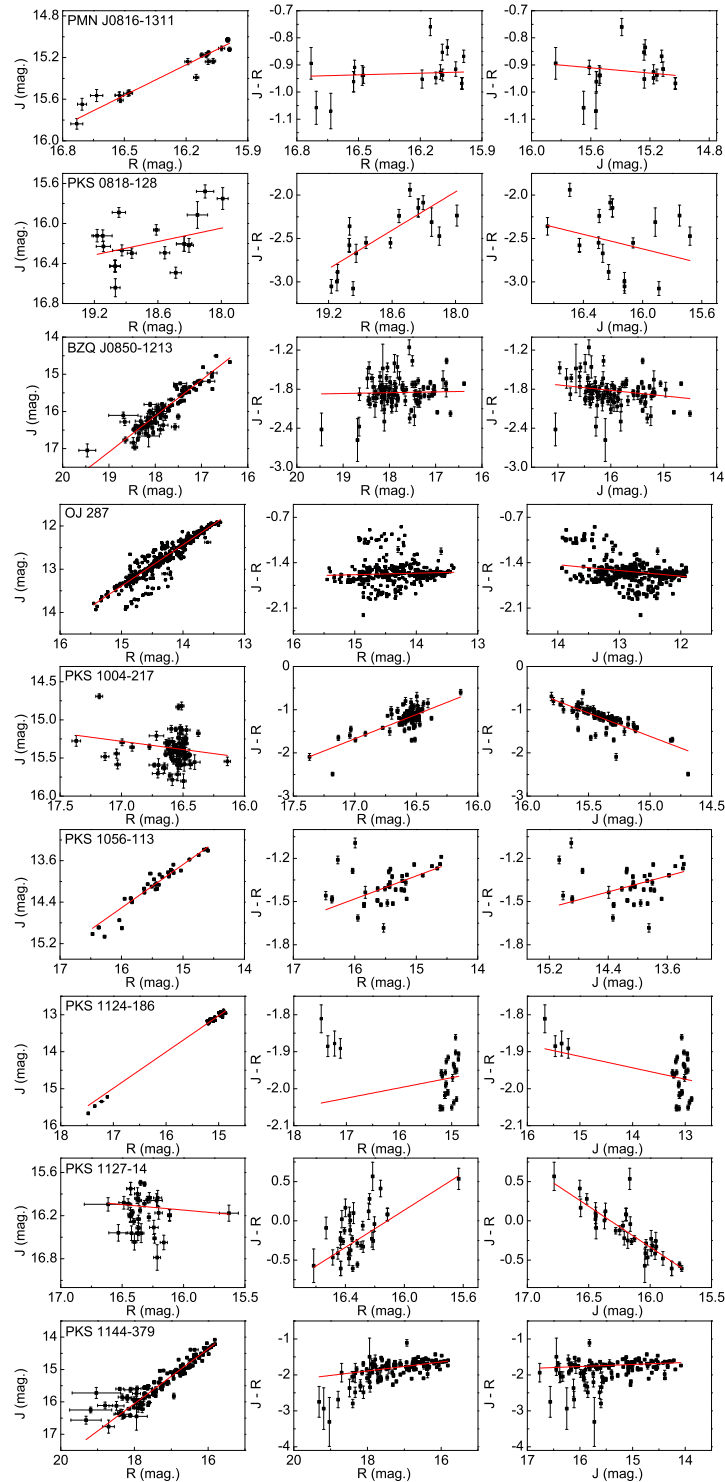
We investigate the correlation between values in the  $R$  and those in the  $J$  bands. The  $R$  band versus  $J$  band is plotted in the left panels in Figure 4. Linear fitting is carried out by the least squares method (the solid lines in the figure). In order to quantitatively search for the relation between these two bands, we calculate the correlation coefficient and estimate the significance level, and list them in Columns 7 and 8 respectively of Table 1. From Figure 4 and the correlation coefficient, one can see that blazars show well-correlated variations between  $R$  and  $J$  bands, except for several sources showing weak, no or even negative correlations.

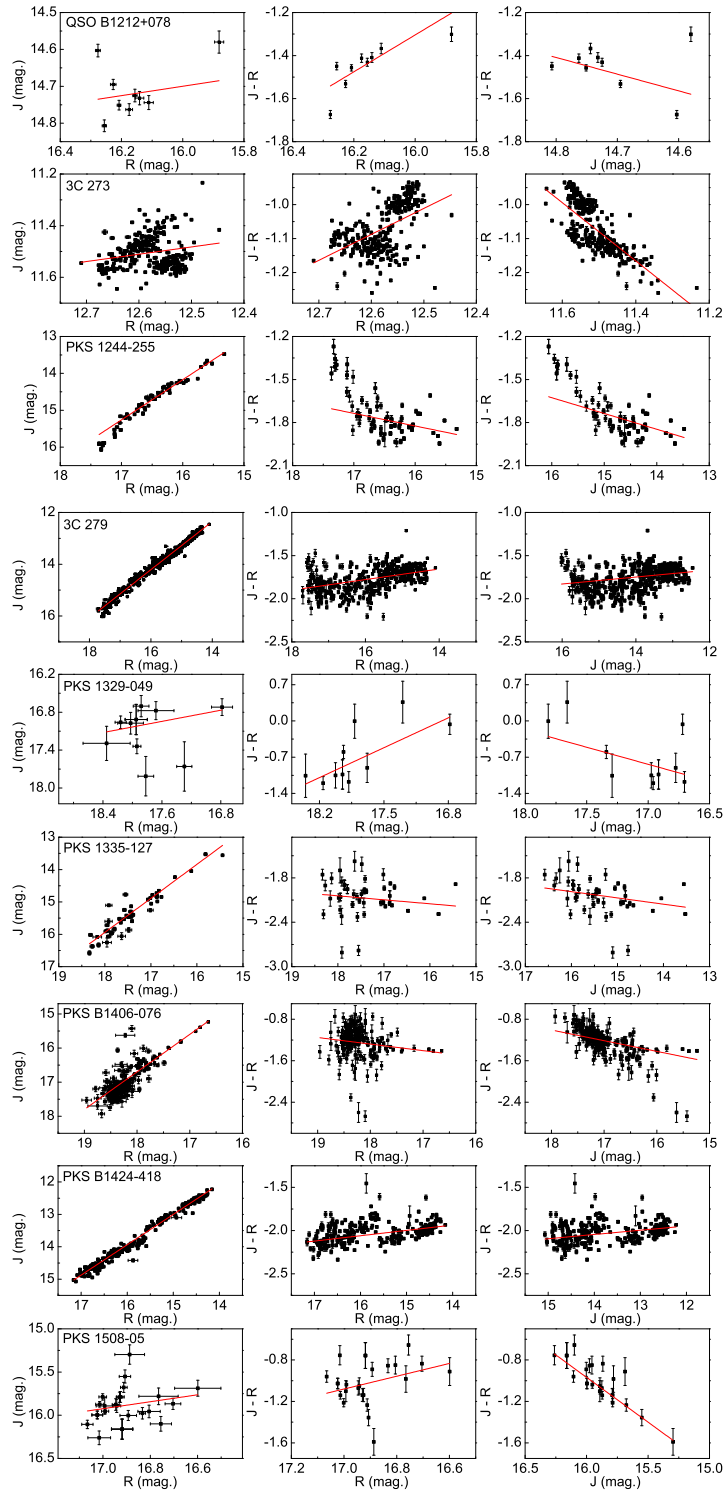


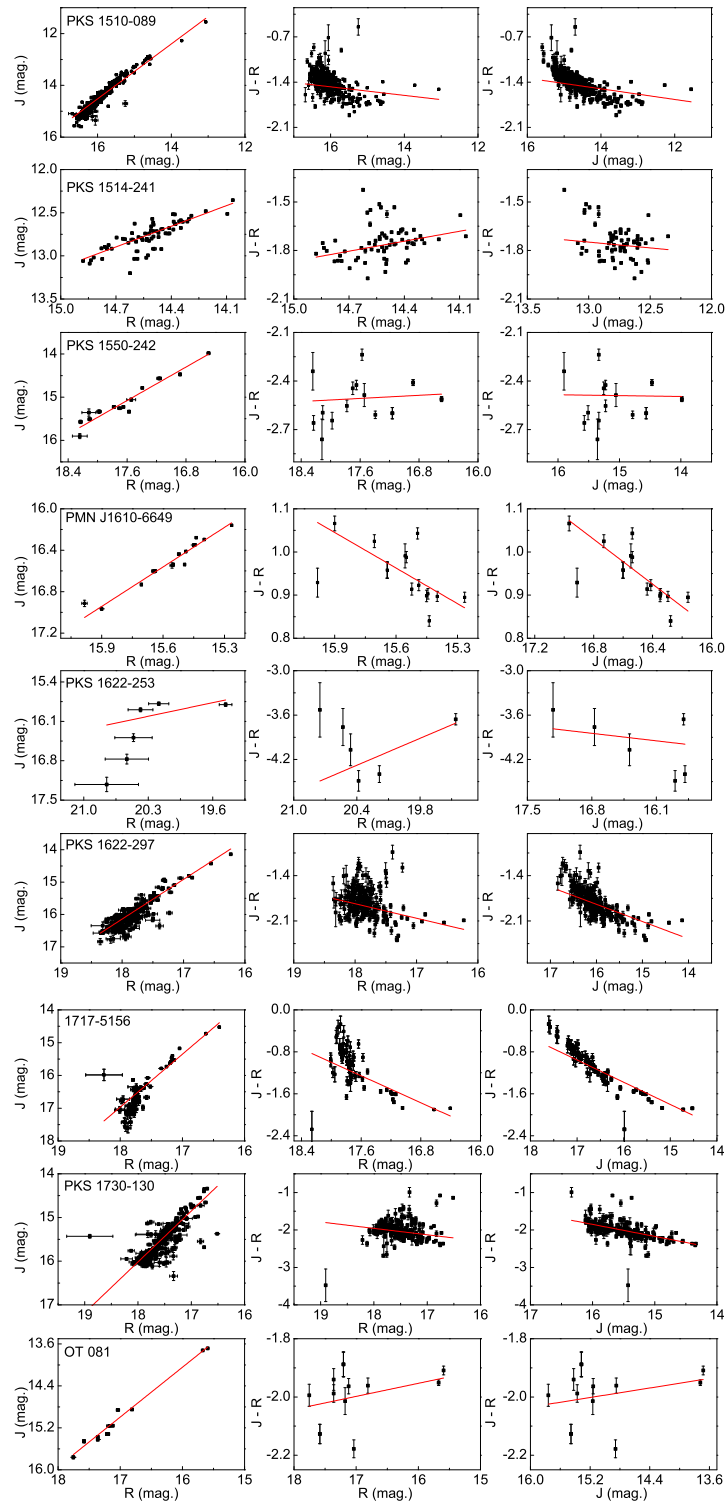
**Fig. 4** *Left:* Relations between the  $J$  and  $R$  magnitudes. *Middle:* Color index vs. the magnitude of  $R$  band. *Right:* Color index versus the magnitude of  $J$  band. The solid lines represent the best linear fitting.

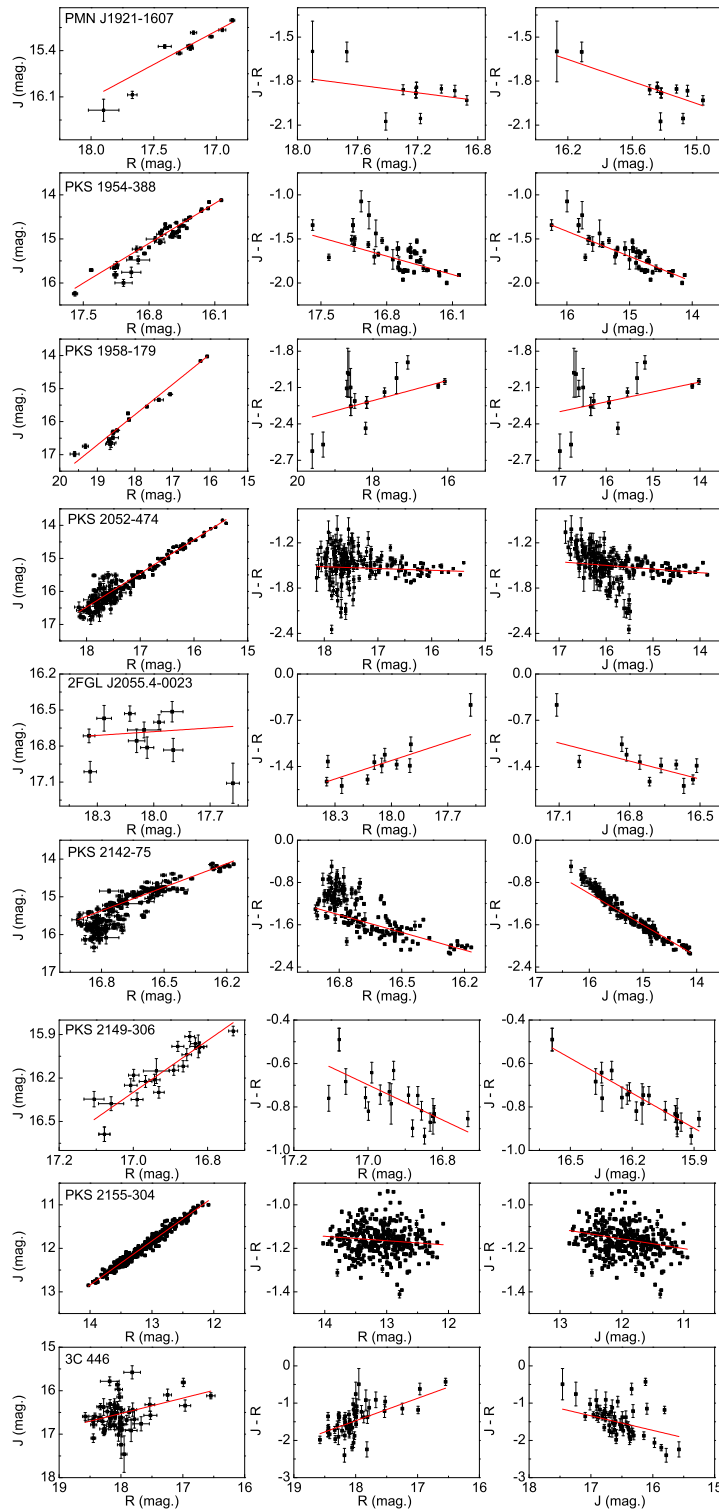
Fig. 4 *Continued.*

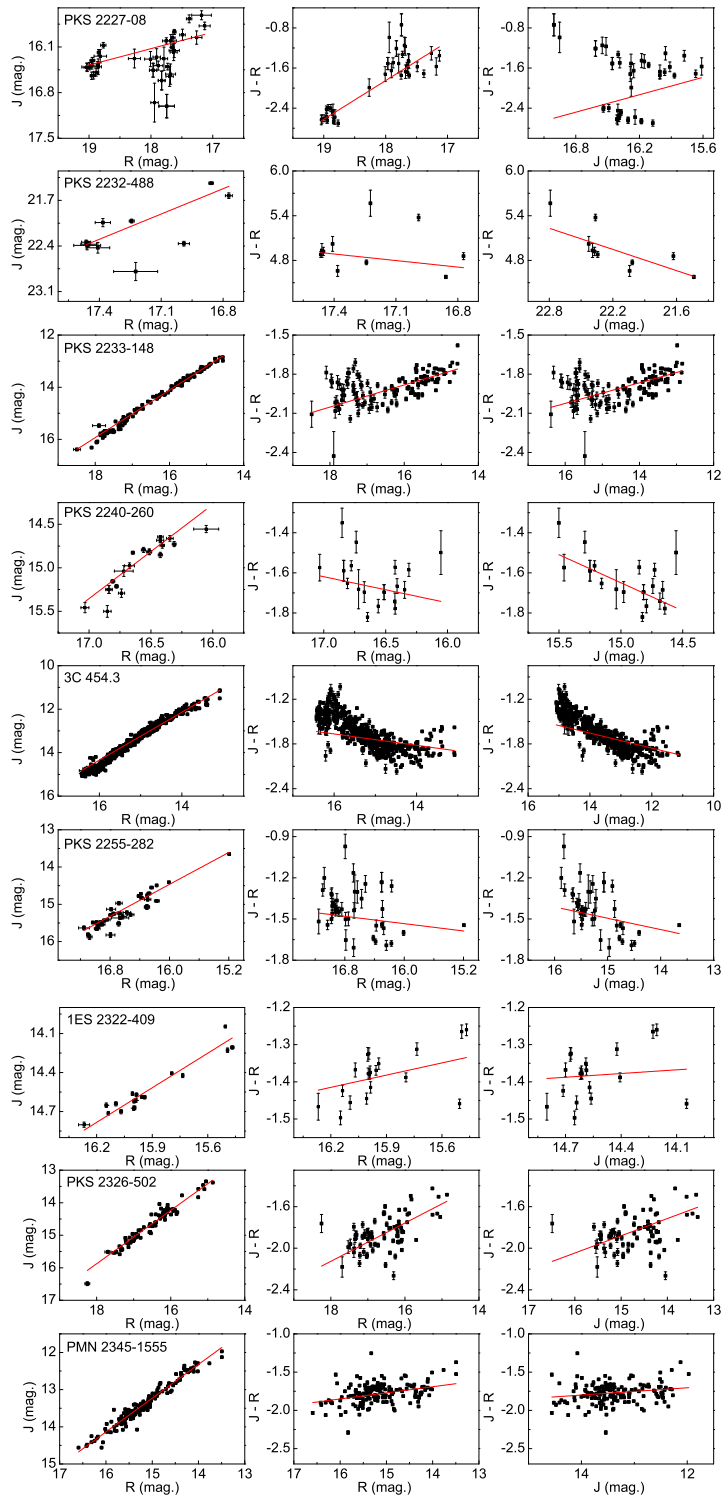
**Fig. 4** *Continued.*

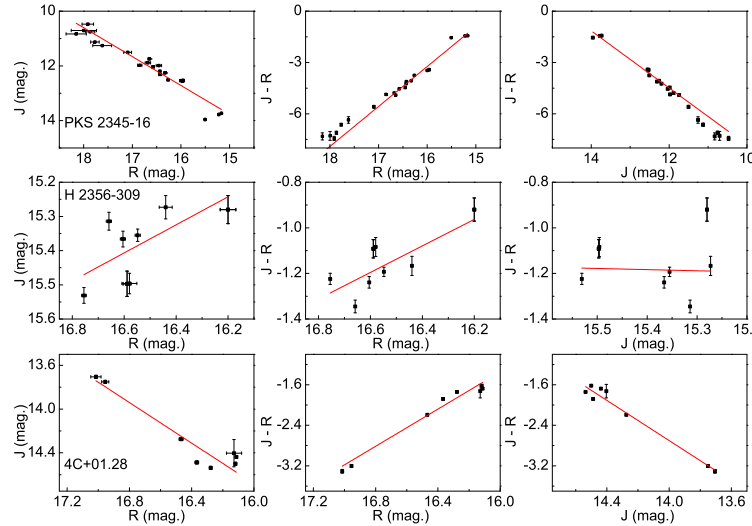
Fig. 4 *Continued.*

Fig. 4 *Continued.*

**Fig. 4** *Continued.*

**Fig. 4** *Continued.*

**Fig. 4** *Continued.*

**Fig. 4** *Continued.*

### 3 COLOR VARIATIONS

The color variability can reflect the spectral variability. Since these sources are highly variable, simultaneous or quasi-simultaneous observations are essential for calculation of the color index. The time series in the optical  $R$  band and the infrared  $J$  band are quasi-simultaneous and are the best representative sample in the SMARTS data. This gives us an opportunity to study the spectral variations of the large sample of blazars on long time scales in detail.  $J - R$  color index is calculated for corresponding pairs between  $R$  and  $J$  bands within the time interval of 15 minutes for each object. More than 90% of intervals are less than 5 minutes. Very few outlying data points were found and later discarded. The middle and right panels of Figure 4 show the  $J - R$  color variations with the brightness in the  $R$  band and  $J$  band, respectively. To obtain the relation between the color index and the source brightness, we calculate the correlation coefficient  $r$  and estimate the significance level. If  $r \geq 0.2$  and the significance level  $p \leq 0.01$ , it means there is a somewhat good correlation between color index and magnitude, which suggests that the source becomes redder when the source becomes brighter. If  $r \leq -0.2$  and the significance level  $p \leq 0.01$ , it means a considerable negative correlation exists and suggests that the source tends to be bluer when the source is brighter. The other cases mean there is no correlation between color index and source brightness. Column 9 of Table 1 lists the correlation coefficient between the color index and the magnitude of the  $R$  band (denoted by  $r_{C-R}$ ). Its significance level is estimated and listed in Column 10. The correlation coefficient between the color index and the magnitude of  $J$  band ( $r_{C-J}$ ) and its significance level are also calculated and listed in Columns 11 and 12 respectively. Overall, 43 sources (35 FSRQs, seven BL Lacs and one unidentified object) show RWB trends and 24 sources (11 FSRQs, 11 BL Lacs and two unidentified objects) show BWB trends. There are 10 sources (six FSRQs and four BL Lacs) showing BWB trends in the *Color-R* plane and opposite trends in the *Color-J* plane. The color behaviors are listed in Column 13 of Table 1.

### 4 DISCUSSION AND CONCLUSIONS

The BWB behavior is usually observed in BL Lac objects, which can usually be explained with shock-in-jet models. This behavior perhaps indicates the presence of two components contributing to the overall emission, a variable component with a constant and relatively blue color and an under-

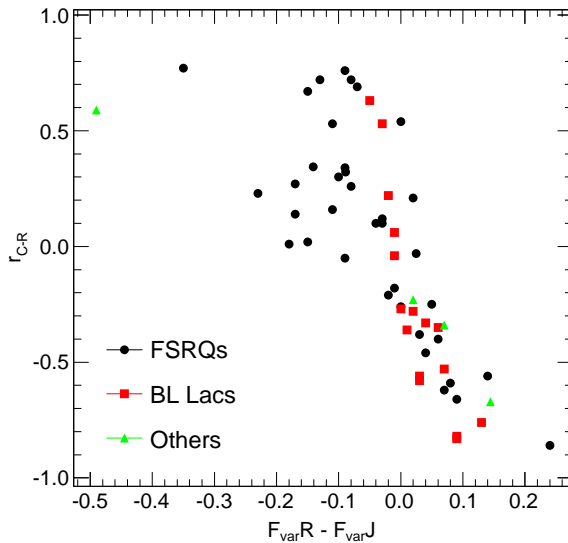


**Fig. 5** Correlation coefficient  $r_{C-R}$  versus the  $F_{\text{var}}$  difference of  $R$  and  $J$  bands.

lying red component (Fiorucci et al. 2004; Ikejiri et al. 2011). RWB behavior is generally observed in FSRQs, which can be interpreted as due to a strong contribution of a blue thermal emission from the accretion disk, which mainly affects the bluer region of the optical spectrum when the jet emission is faint (Villata et al. 2006; Rani et al. 2010; Bonning et al. 2012).

An interesting result is that 10 sources show one color behavior in one band and an opposite trend in the other band. When the  $R$  band (higher frequency) brightness increases, there tend to be BWB trends. However, the RWB behavior tends to appear when the source brightness increases in the  $J$  band (lower frequency). This phenomenon has even clearly appeared in the case of 3C 273 (Dai et al. 2009). This may be caused by the brightness variations in the higher frequency leading those in the lower frequency. In other words, the radiation emitted at higher frequencies will emerge sooner while the maximum flux at lower frequencies will be observed later (Villata et al. 2000; Papadakis et al. 2004; Villata et al. 2009; Zhang et al. 2010b; Rani et al. 2010). Thus the variations in lower frequencies cannot keep step with those in high frequencies. One would observe weak, none or even negative correlations between the two bands. Therefore, the object exhibits the BWB trend in the higher frequency band but the RWB trend in the lower frequency band. We check the brightness correlations between  $J$  and  $R$  bands, and find that the correlations are weak or negative for these sources.

For sources with strong brightness correlations between  $R$  and  $J$  bands, their color behaviors in the  $R$  band are similar to those in the  $J$  band, showing either BWB or RWB behavior. We investigate the relation between color behavior and  $F_{\text{var}}$  difference of  $R$  and  $J$  bands for those objects with an absolute value of  $r_{J-R}$  greater than 0.5.

In Figure 5, we plot the  $r_{C-R}$  versus the  $F_{\text{var}}$  difference,  $F_{\text{var}R} - F_{\text{var}J}$ . Overall, if  $F_{\text{var}}$  of the  $R$  band is greater than that of the  $J$  band,  $r_{C-R} < 0$ , it means the source shows the BWB trend. If  $F_{\text{var}}$  of the  $R$  band is less than that of the  $J$  band, the source shows the RWB trend ( $r_{C-R} > 0$ ). This means that the difference in variation amplitude can cause different color behaviors. For an object with fluxes at different frequencies varying simultaneously, if the amplitude is larger at the higher frequency than at the lower one, it exhibits the BWB trend. Correspondingly, the larger amplitude variations at lower frequency can result in the RWB trend.

From Figure 4, one can see that not all sources can be fitted well by a straight line. The color variations of some sources may change trend at a certain magnitude. Several sources show RWB in the low state, and then keep a stable trend in the high state (SWB), such as PMN 0017–0512, PKS 0208–512, PKS 1244–255, PKS 1510–089, PKS 1622–297 and 1717–5156. Similarly, some sources show a RWB trend in the low state, and a BWB trend in the high state, like AO 0235+164, PKS 1056–113, PKS 2233–148, PKS 2240–260 and 3C 454.3. This behavior has also been found in other literature, such as 3C 454.3, PKS 1510–089, PG 1553+113 and PKS 0537–441 in Villata et al. (2006), Ikejiri et al. (2011) and Zhang et al. (2013). Most of these sources are FSRQs. They have a common feature that they exhibit an RWB trend in the faint state and then an SWB or BWB trend in the bright state. This may be explained as a reversal in the contribution of different emission components. In the faint state, the strong contribution of thermal emission from an accretion disk results in the RWB trend. However in the bright state, the non-thermal jet emission is dominant, which would display the usual BWB trend, therefore balancing or exceeding the RWB trend. Thus, the source transforms its color behavior from the RWB trend to the SWB or BWB trend.

A few sources show two or more different trends in the *Magnitude-Magnitude* or *Color-Magnitude* diagrams. PKS 0426–380 clearly shows two different behaviors. In the  $J - R$  diagram, there seems to be a gap between two light curves with different heights on the graph. In the *Color-Magnitude* diagram, there is also an intersection of two curves. One exhibits the BWB trend, and the other exhibits the RWB trend. OJ 287 indicates two parts in the color behavior and the data points are very scattered. The color seems to show no trend in the *Color-R* diagram, however, it shows a slight RWB trend in the *Color-J* diagram. The BWB trend had been found in this source (Vagnetti et al. 2003; Fiorucci et al. 2004; Wu et al. 2006; Dai et al. 2011). A tendency to move around a circle in the *Color-Magnitude* diagram was also found by Bonning et al. (2012) and Sandrinelli et al. (2014). For 3C 273, the  $J - R$  plot shows two separate parts and the *Color-Magnitude* plot also shows two separate parts. Two parts both have a RWB trend, and the whole *Color-J* shows the RWB trend. However, in the *Color-R* plot, the combination of the two parts shows the BWB trend. Very recently, Fan et al. (2014) also found that this source exhibited two separate parts in the plot of spectral index versus flux density. PKS 2052–474 seems to display two different behaviors in the variations that both have RWB trends. PKS 2227–08 shows two separate parts, which both show a RWB trend. However, the combination of these two parts shows a BWB trend in the *Color-R* plot. These color behaviors are puzzling, which suggest that there are possibly more complicated and separate emission components in these sources.

In conclusion, the color variability has been investigated with a large sample of blazars in the optical and infrared region. On the whole, 46 out of 49 FSRQs show color variations with RWB trends (35 FSRQs) or BWB trends (11 FSRQs), and 18 out of 22 BL Lacs show RWB trends (seven BL Lacs) or BWB trends (11 BL Lacs). Among them, 10 blazars follow the RWB trend in the faint state and then the SWB or BWB trend in the bright state.

**Acknowledgements** We express our thanks to the referee for great help. This work has been supported by the National Natural Science Foundation of China (Grant No. 11273008), and partly by the Foundation for Young Talents in College of Anhui Province (Grant No. 2012SQRL116). This paper has made use of up-to-date SMARTS optical/near-infrared light curves that are available at [www.astro.yale.edu/smarts/glast/home.php](http://www.astro.yale.edu/smarts/glast/home.php).

## References

- Arévalo, P., Uttley, P., Kaspi, S., et al. 2008, MNRAS, 389, 1479
- Bonning, E., Urry, C. M., Bailyn, C., et al. 2012, ApJ, 756, 13
- Carini, M. T., Miller, H. R., Noble, J. C., & Goodrich, B. D. 1992, AJ, 104, 15
- Chatterjee, R., Bailyn, C. D., Bonning, E. W., et al. 2012, ApJ, 749, 191

- Ciprini, S., Takalo, L. O., Tosti, G., et al. 2007, A&A, 467, 465  
 Dai, B. Z., Li, X. H., Liu, Z. M., et al. 2009, MNRAS, 392, 1181  
 Dai, Y., Wu, J., Zhu, Z.-H., Zhou, X., & Ma, J. 2011, AJ, 141, 65  
 D'Ammando, F., Antolini, E., Tosti, G., et al. 2013, MNRAS, 431, 2481  
 Fan, J. H., Kurtanidze, O., Liu, Y., et al. 2014, ApJS, 213, 26  
 Fan, J. H., & Lin, R. G. 2000, ApJ, 537, 101  
 Fiorucci, M., Ciprini, S., & Tosti, G. 2004, A&A, 419, 25  
 Gaur, H., Gupta, A. C., Strigachev, A., et al. 2012, MNRAS, 425, 3002  
 Ghosh, K. K., Ramsey, B. D., Sadun, A. C., & Soundararajaperumal, S. 2000, ApJS, 127, 11  
 Gu, M.-F., & Ai, Y. L. 2011, A&A, 528, A95  
 Gu, M. F., Lee, C.-U., Pak, S., Yim, H. S., & Fletcher, A. B. 2006, A&A, 450, 39  
 Hu, S. M., Wu, J. H., Zhao, G., & Zhou, X. 2006, MNRAS, 373, 209  
 Ikejiri, Y., Uemura, M., Sasada, M., et al. 2011, PASJ, 63, 639  
 Papadakis, I. E., Boumis, P., Samaritakis, V., & Papamastorakis, J. 2003, A&A, 397, 565  
 Papadakis, I. E., Samaritakis, V., Boumis, P., & Papamastorakis, J. 2004, A&A, 426, 437  
 Raiteri, C. M., Villata, M., Tosti, G., et al. 2003, A&A, 402, 151  
 Rani, B., Gupta, A. C., Strigachev, A., et al. 2010, MNRAS, 404, 1992  
 Sandrinelli, A., Covino, S., & Treves, A. 2014, A&A, 562, A79  
 Vagnetti, F., Trevese, D., & Nesci, R. 2003, ApJ, 590, 123  
 Vaughan, S., Edelson, R., Warwick, R. S., & Uttley, P. 2003, MNRAS, 345, 1271  
 Villata, M., Mattox, J. R., Massaro, E., et al. 2000, A&A, 363, 108  
 Villata, M., Raiteri, C. M., Balonek, T. J., et al. 2006, A&A, 453, 817  
 Villata, M., Raiteri, C. M., Larionov, V. M., et al. 2009, A&A, 501, 455  
 Wu, J., Zhou, X., Ma, J., & Jiang, Z. 2011, MNRAS, 418, 1640  
 Wu, J., Zhou, X., Wu, X.-B., et al. 2006, AJ, 132, 1256  
 Zhang, B.-K., Dai, B.-Z., Zhang, L., & Cao, Z. 2010a, RAA (Research in Astronomy and Astrophysics), 10, 653  
 Zhang, B., Dai, B., Zhang, L., Liu, J., & Cao, Z. 2010b, PASA, 27, 296  
 Zhang, B.-K., Wang, S., Zhao, X.-Y., Dai, B.-Z., & Zha, M. 2013, MNRAS, 428, 3630  
 Zhang, B.-K., Zhao, X.-Y., Wang, C.-X., & Dai, B.-Z. 2014, RAA (Research in Astronomy and Astrophysics), 14, 933